Supplement of Atmos. Chem. Phys., 19, 15609–15628, 2019
https://doi.org/10.5194/acp-19-15609-2019-supplement

Atmospheric Chemistry and Physics
Open Access

Supplement of

Sources and formation of carbonaceous aerosols in Xi'an, China: primary emissions and secondary formation constrained by radiocarbon

Haiyan Ni et al.

Correspondence to: Ru-Jin Huang (rujin.huang@ieecas.cn)

S1. Sensitivity study for potential pyrolysis effects on $\delta^{13}C_{EC}$

In this study, we used a two-step method (OC step: 375 °C for 3 h; EC step: 850 °C for 5 h) to isolate OC and EC for $\delta^{13}C$ analysis, as described in Sect. 2.3. Our earlier study in Xi'an found that EC recovery for $\delta^{13}C$ analysis (relative to EC quantified by the thermal-optical reflectance protocol IMPROVE_A; Chow et al., 2007) was on average 123 ± 8 %, higher than 100% (Zhao et al., 2018). The reason is that pyrolyzed OC (formed through charring during the OC removal procedure) and possibly some remaining OC compounds (e.g., high molecular weight refractory carbon) can be released at the high temperature of the EC step.

The resulted $\delta^{13}C$ of EC could be biased by $\delta^{13}C$ of pyrolyzed OC, if the contribution from pyrolyzed OC to the isolated EC is high and $\delta^{13}C$ of pyrolyzed OC is very different from $\delta^{13}C$ of pure EC. To examine the effect of pyrolyzed OC on $\delta^{13}C$ of EC, a sensitivity analysis is performed. $\delta^{13}C$ of pyrolyzed OC is not known, but our recent studies suggest that $\delta^{13}C$ of pyrolyzed OC is not very different from $\delta^{13}C_{OC}$ (<1‰ in many cases). We thus use $\delta^{13}C_{OC}$ to represent $\delta^{13}C$ of pyrolyzed OC. $\delta^{13}C$ of pure EC is calculated based on isotope mass balance. This analysis shows that for high contribution from pyrolyzed OC to the isolated EC of 20%, the expected difference in $\delta^{13}C$ between measured EC and true EC is still <1‰. This will not significantly change any conclusions made in this study.

S2. Estimation of the probability density functions (PDFs) of *p* values

The p value used in Eq. (11) in the main text is the fraction of EC from coal combustion (EC_{coal}) in EC from fossil sources (EC_{fossil}). That is,

$$p = \frac{\mathrm{EC_{coal}}}{\mathrm{EC_{fossil}}} = \frac{\mathrm{EC_{coal}}}{\mathrm{EC_{coal}} + \mathrm{EC_{liq.fossil}}} \tag{S1}$$

where EC_{fossil} is the sum of EC_{coal} and EC from liquid fossil fuel combustion (i.e., vehicle emissions; $EC_{liq.fossil}$).

Eq. (S1) can be formulated as:

$$p = \frac{f_{\mathrm{coal}}}{f_{\mathrm{fossil}}} = \frac{f_{\mathrm{coal}}}{f_{\mathrm{coal}} + f_{\mathrm{liq.fossil}}} \tag{S2}$$

where f_{coal} and $f_{liq.fossil}$ is the relative contribution of coal combustion emission and liquid fossil fuel combustion to EC. The sum of f_{coal} and $f_{liq.fossil}$ is f_{fossil} of EC, which is well constrained by $F^{14}C$ of EC.

The PDFs of f_{coal} and $f_{liq.fossil}$ (eg., Fig. 6 in the main text), derived from the Bayesian calculations detailed in Sect. 2.6 in the main text, are used to calculated the PDFs of p.

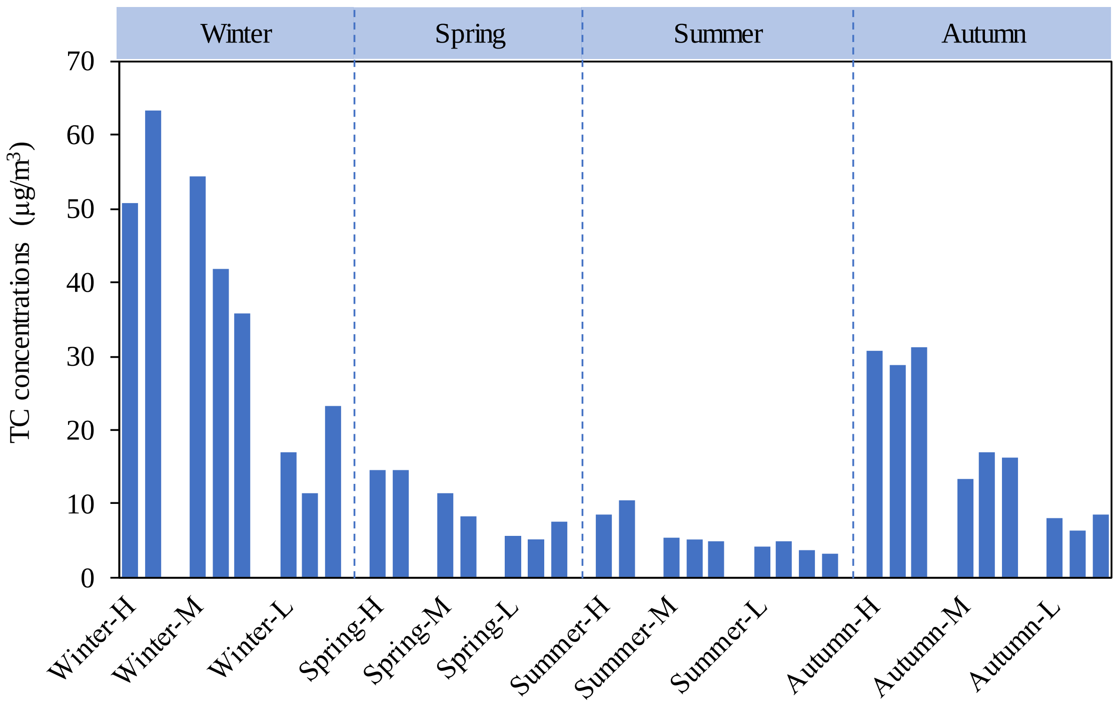

Figure S1. Selected samples for ^{14}C analysis. Three composite samples that represent high (H), medium (M) and low (L) TC concentrations are combined from several individual filter samples per season. Each composite sample is consisting of 2 to 4 24-hr filter pieces with similar TC loadings and air mass backward trajectories (Table S1).

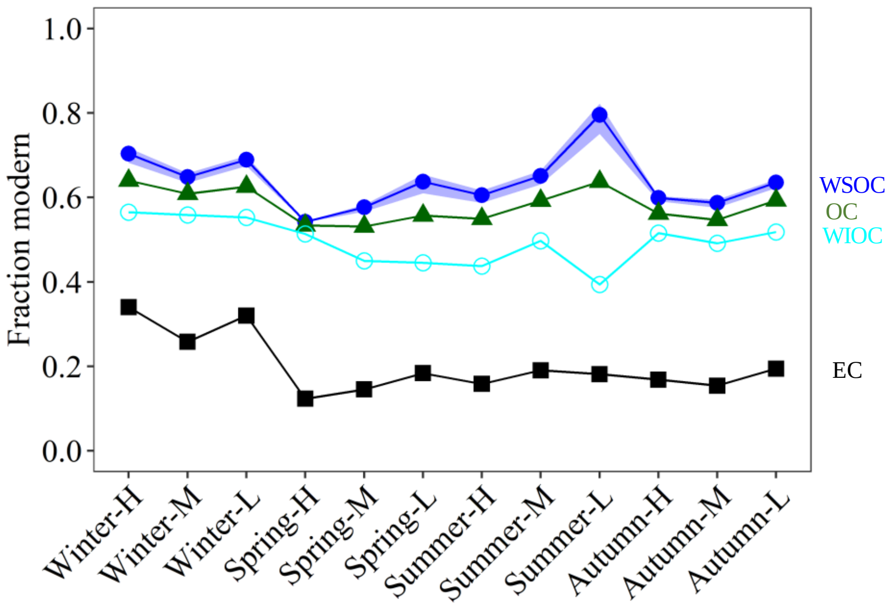

Figure S2. Fraction modern ($F^{14}C$) of elemental carbon (EC), organic carbon (OC), water-insoluble OC (WIOC) and water-soluble OC (WSOC) ($F^{14}C_{(EC)}$, $F^{14}C_{(OC)}$, $F^{14}C_{(WIOC)}$ and $F^{14}C_{(WSOC)}$ respectively). $F^{14}C_{(WSOC)}$ is calculated from the measured $F^{14}C_{(OC)}$ and $F^{14}C_{(WIOC)}$ following the isotope mass balance. The blue dashed area for best estimate of $F^{14}C_{(WSOC)}$ (blue filled circle) indicates ranges of $F^{14}C_{(WSOC)}$ (Sect. 2.5).

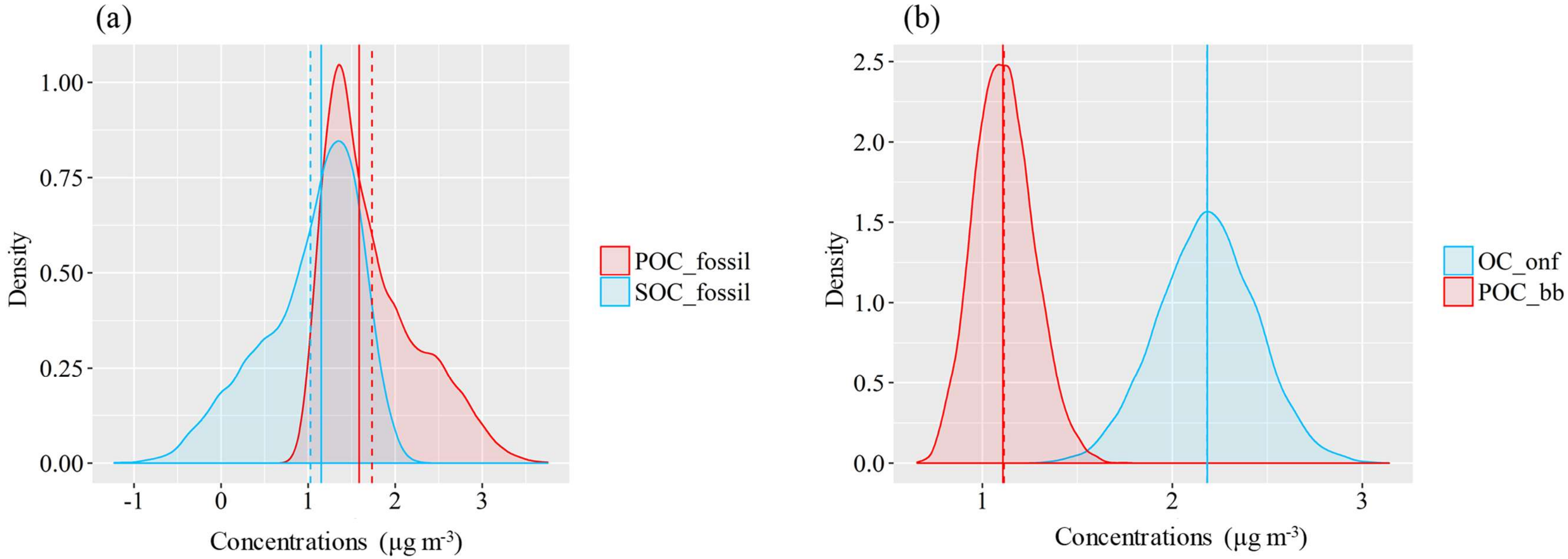

Figure S3. **(a)** Example probability density functions (PDFs) of concentrations of POC_{fossil} (red), SOC_{fossil} (light blue) for sample Autumn-L. **(b)** PDFs of concentrations of $OC_{o,nf}$ (light blue) and POC_{bb} (red) for the same sample. Their concentrations are estimated by ^{14}C-apportioned OC and EC using the EC tracer method (Sect. 2.5). The mean and median are indicated by the dashed and solid vertical lines.

Table S1. Sample information as well as the fraction modern ($F^{14}C$) of elemental carbon (EC), organic carbon (OC), water-insoluble OC (WIOC) and water-soluble OC (WSOC) ($F^{14}C_{(EC)}$, $F^{14}C_{(OC)}$, $F^{14}C_{(WIOC)}$ and $F^{14}C_{(WSOC)}$ respectively), and stable carbon isotopic compositions ($\delta^{13}C$, ‰) of EC ($\delta^{13}C_{EC}$).

Sample name	Sampling Date (month/day/year)	$F^{14}C_{(EC)}$[a]	$F^{14}C_{(OC)}$[a]	$F^{14}C_{(WIOC)}$[a]	$F^{14}C_{(WSOC)}$[b]	$\delta^{13}C_{EC}$
Winter-H	12/20/2015 12/21/2015	0.340 ± 0.005	0.640 ± 0.009	0.565 ± 0.006	0.704 (0.682–0.717)	-24.64 ± 0.02
Winter-M	11/30/2015 12/8/2015 12/9/2015	0.258 ± 0.005	0.609 ± 0.007	0.558 ± 0.007	0.649 (0.635–0.657)	-25.04 ± 0.04
Winter-L	12/14/2015 12/16/2015 12/17/2015	0.320 ± 0.005	0.626 ± 0.007	0.553 ± 0.006	0.69 (0.675–0.699)	-24.71 ± 0.02
Spring-H	5/5/2016 5/10/2016	0.123 ± 0.004	0.534 ± 0.006	0.514 ± 0.006	0.543 (0.541–0.543)	-24.66 ± 0.04
Spring-M	4/19/2016 4/20/2016	0.145 ± 0.006	0.531 ± 0.007	0.450 ± 0.006	0.577 (0.567–0.583)	-24.77 ± 0.02
Spring-L	4/23/2016 4/24/2016 4/27/2016	0.184 ± 0.004	0.557 ± 0.007	0.445 ± 0.006	0.637 (0.610–0.654)	-24.24 ± 0.02
Summer-H	7/21/2016 7/23/2016	0.159 ± 0.004	0.549 ± 0.006	0.438 ± 0.006	0.605 (0.587–0.616)	-24.67 ± 0.02
Summer-M	7/11/2016 7/16/2016 7/27/2016	0.191 ± 0.004	0.593 ± 0.007	0.497 ± 0.006	0.651 (0.631–0.663)	-25.25 ± 0.09
Summer-L	7/5/2016 7/6/2016 7/12/2016 7/13/2016	0.181 ± 0.006	0.637 ± 0.007	0.394 ± 0.006	0.795 (0.750–0.822)	-24.96 ± 0.02
Autumn-H	11/3/2016 11/4/2016 11/13/2016	0.169 ± 0.004	0.562 ± 0.007	0.516 ± 0.007	0.599 (0.591–0.603)	-25.24 ± 0.04
Autumn-M	10/17/2016 10/18/2016 11/1/2016	0.154 ± 0.004	0.547 ± 0.007	0.492 ± 0.006	0.587 (0.575–0.595)	-25.51 ± 0.03
Autumn-L	10/15/2016 10/16/2016 10/20/2016	0.194 ± 0.004	0.593 ± 0.006	0.518 ± 0.006	0.635 (0.623–0.643)	-25.10 ± 0.02

[a] $F^{14}C$ values are given in average ± measurement uncertainty.
[b] $F^{14}C_{(WSOC)}$ is calculated from the measured $F^{14}C_{(OC)}$ and $F^{14}C_{(WIOC)}$ following the isotope mass balance (Eq. 4 in the main text). The range of $F^{14}C_{(WSOC)}$ is presented in the parentheses, calculated following the method detailed in Sect 2.5.

Table S2. Consensus value of $F^{14}C$ for secondary standards IAEA- C7 and -C8 along with measured $F^{14}C$ values. Data corrections for the measured $F^{14}C$ of secondary standards are the same as those for samples.

Standards	Consensus value of $F^{14}C$	measured $F^{14}C$	measured mass (μgC)
IAEA-C7	0.4953 ± 0.0012	0.4884 ± 0.0059	76
		0.5017 ± 0.0064	80
IAEA-C8	0.1503 ± 0.0017	0.1511 ± 0.0039	63
		0.1540 ± 0.0038	100

Table S3. Concentrations of EC, OC, WIOC and WSOC from non-fossil sources (EC_{bb}, OC_{nf}, $WIOC_{nf}$ and $WSOC_{nf}$) and fossil sources (EC_{fossil}, OC_{fossil}, $WIOC_{fossil}$ and $WSOC_{fossil}$) in units of μg m^{-3} for each sample.

Sample name	EC_{bb}	EC_{fossil}	OC_{nf}	OC_{fossil}	$WIOC_{nf}$	$WIOC_{fossil}$	$WSOC_{nf}$	$WSOC_{fossil}$
Winter-H	3.08 ± 0.18	6.86 ± 0.39	27.66 ± 1.56	19.43 ± 1.20	10.78 ± 0.78	10.12 ± 0.74	16.72 ± 1.82	9.43 ± 1.08
Winter-M	1.44 ± 0.09	4.70 ± 0.28	21.17 ± 1.17	16.73 ± 0.97	8.25 ± 0.62	7.95 ± 0.59	12.80 ± 1.36	8.89 ± 0.96
Winter-L	0.82 ± 0.06	1.99 ± 0.14	8.31 ± 0.48	6.16 ± 0.37	3.33 ± 0.17	3.27 ± 0.17	4.95 ± 0.53	2.94 ± 0.32
Spring-H	0.36 ± 0.03	2.86 ± 0.19	5.62 ± 0.33	5.85 ± 0.34	1.56 ± 0.08	1.77 ± 0.09	4.03 ± 0.33	4.12 ± 0.34
Spring-M	0.30 ± 0.03	2.00 ± 0.15	3.68 ± 0.22	3.87 ± 0.23	1.08 ± 0.06	1.56 ± 0.08	2.58 ± 0.24	2.34 ± 0.22
Spring-L	0.22 ± 0.02	1.09 ± 0.10	2.48 ± 0.16	2.37 ± 0.15	0.79 ± 0.06	1.15 ± 0.09	1.68 ± 0.19	1.23 ± 0.14
Summer-H	0.32 ± 0.03	1.88 ± 0.14	3.71 ± 0.23	3.65 ± 0.22	0.94 ± 0.08	1.41 ± 0.11	2.75 ± 0.26	2.25 ± 0.21
Summer-M	0.17 ± 0.02	0.83 ± 0.08	2.25 ± 0.15	1.89 ± 0.13	0.68 ± 0.06	0.82 ± 0.07	1.55 ± 0.17	1.07 ± 0.12
Summer-L	0.12 ± 0.02	0.60 ± 0.07	1.96 ± 0.14	1.39 ± 0.10	0.46 ± 0.03	0.82 ± 0.05	1.49 ± 0.17	0.58 ± 0.08
Autumn-H	1.05 ± 0.07	5.79 ± 0.33	12.05 ± 0.68	11.32 ± 0.64	4.77 ± 0.22	5.37 ± 0.24	7.22 ± 0.72	6.03 ± 0.61
Autumn-M	0.54 ± 0.04	3.29 ± 0.21	5.88 ± 0.35	5.83 ± 0.35	2.13 ± 0.15	2.62 ± 0.18	3.71 ± 0.38	3.24 ± 0.34
Autumn-L	0.28 ± 0.02	1.29 ± 0.11	3.29 ± 0.21	2.76 ± 0.18	0.99 ± 0.07	1.11 ± 0.08	2.29 ± 0.23	1.67 ± 0.17

Table S4. Concentrations (μg m^{-3}) of primary OC from biomass burning (POC_{bb}), OC from non-fossil sources excluding primary biomass burning ($OC_{o,nf}$), primary OC from fossil sources (POC_{fossil}), secondary OC from fossil sources (SOC_{fossil}) (median and interquartile range). The median values for POC_{bb} and $OC_{o,nf}$ are very close to their mean values due to their symmetric PDFs (Fig. S3b).

Sample Name	POC_{bb}	$OC_{o.nf}$	POC_{fossil}	SOC_{fossil}
Winter-H	12.27 (11.26–13.37)	15.34 (13.87–16.78)	9.24 (7.52–11.64)	10.10 (7.64–11.97)
Winter-M	5.77 (5.26–6.27)	15.37 (14.45–16.29)	5.99 (4.95–7.70)	10.55 (8.92–11.84)
Winter-L	3.26 (2.98–3.55)	5.03 (4.61–5.46)	2.69 (2.19–3.39)	3.42 (2.73–3.99)
Spring-H	1.44 (1.31–1.58)	4.17 (3.92–4.42)	3.87 (3.05–5.05)	1.97 (0.81–2.77)
Spring-M	1.22 (1.11–1.33)	2.46 (2.27–2.64)	2.58 (2.10–3.34)	1.28 (0.52–1.77)
Spring-L	0.87 (0.79–0.96)	1.60 (1.46–1.74)	1.58 (1.25–1.98)	0.77 (0.38–1.12)
Summer-H	1.26 (1.15–1.38)	2.45 (2.26–2.64)	2.49 (2.00–3.22)	1.15 (0.42–1.66)
Summer-M	0.69 (0.62–0.77)	1.55 (1.43–1.67)	1.00 (0.84–1.25)	0.87 (0.60–1.06)
Summer-L	0.47 (0.42–0.53)	1.48 (1.38–1.59)	0.76 (0.62–0.98)	0.62 (0.40–0.78)
Autumn-H	4.20 (3.84–4.56)	7.88 (7.30–8.45)	7.07 (5.93–9.06)	4.21 (2.21–5.43)
Autumn-M	2.14 (1.96–2.34)	3.73 (3.43–4.03)	3.75 (3.23–4.78)	2.02 (0.99–2.61)
Autumn-L	1.11 (1.00–1.22)	2.18 (2.01–2.35)	1.61 (1.34–2.05)	1.13 (0.68–1.43)

Table S5. Relative non-fossil sources contribution to EC, OC, WIOC and WSOC (f_{bb}(EC), f_{nf}(OC), f_{nf}(WIOC), f_{nf}(WSOC)), and relative fossil sources contribution to EC, OC, WIOC and WSOC (f_{fossil}(EC), f_{fossil}(OC), f_{fossil}(WIOC), f_{fossil}(WSOC)) in different seasons and throughout the year.

Season	f_{bb}(EC)	f_{fossil}(EC)	f_{nf}(OC)	f_{fossil}(OC)	f_{nf}(WIOC)	f_{fossil}(WIOC)	f_{nf}(WSOC)	f_{fossil}(WSOC)
Winter	0.279 ± 0.039	0.721 ± 0.039	0.573 ± 0.014	0.427 ± 0.014	0.510 ± 0.006	0.490 ± 0.006	0.619 ± 0.026	0.381 ± 0.026
Spring	0.137 ± 0.028	0.863 ± 0.028	0.496 ± 0.013	0.504 ± 0.013	0.428 ± 0.035	0.572 ± 0.035	0.533 ± 0.042	0.467 ± 0.042
Summer	0.161 ± 0.015	0.839 ± 0.015	0.544 ± 0.040	0.456 ± 0.040	0.404 ± 0.047	0.596 ± 0.047	0.620 ± 0.089	0.380 ± 0.089
Autumn	0.157 ± 0.019	0.843 ± 0.019	0.521 ± 0.021	0.479 ± 0.021	0.464 ± 0.013	0.536 ± 0.013	0.552 ± 0.023	0.448 ± 0.023
Annual	0.183 ± 0.062	0.817 ± 0.062	0.534 ± 0.037	0.466 ± 0.037	0.451 ± 0.049	0.549 ± 0.049	0.581 ± 0.060	0.419 ± 0.060

Table S6. Concentrations of EC, OC, WIOC and WSOC from non-fossil sources (EC_{bb}, OC_{nf}, $WIOC_{nf}$ and $WSOC_{nf}$) and fossil sources (EC_{fossil}, OC_{fossil}, $WIOC_{fossil}$ and $WSOC_{fossil}$) in units of μg m^{-3} in different seasons and throughout the year.

Season	EC_{bb}	EC_{fossil}	OC_{nf}	OC_{fossil}	$WIOC_{nf}$	$WIOC_{fossil}$	$WSOC_{nf}$	$WSOC_{fossil}$
Winter	1.78 ± 1.17	4.52 ± 2.44	19.05 ± 9.85	14.11 ± 7.01	7.45 ± 3.79	7.11 ± 3.50	11.49 ± 5.99	7.09 ± 3.60
Spring	0.29 ± 0.07	1.98 ± 0.89	3.93 ± 1.58	4.03 ± 1.75	1.14 ± 0.39	1.49 ± 0.31	2.76 ± 1.18	2.56 ± 1.46
Summer	0.20 ± 0.10	1.10 ± 0.68	2.64 ± 0.94	2.31 ± 1.19	0.69 ± 0.24	1.02 ± 0.34	1.93 ± 0.71	1.30 ± 0.86
Autumn	0.62 ± 0.39	3.46 ± 2.25	7.07 ± 4.50	6.64 ± 4.34	2.63 ± 1.94	3.03 ± 2.16	4.41 ± 2.54	3.65 ± 2.21
Annual	0.72 ± 0.84	2.76 ± 2.03	8.17 ± 8.23	6.77 ± 5.94	2.98 ± 3.34	3.16 ± 3.06	5.15 ± 4.85	3.65 ± 2.97

Table S7. Fractional contribution of different incomplete combustion sources to EC in different seasons (median, interquartile range (25th-75th percentile)).

Sources		Winter	Spring	Summer	Autumn
Biomass burning	median	0.28	0.146	0.163	0.159
	25th-75th percentile	(0.26–0.31)	(0.13–0.17)	(0.15–0.18)	(0.15–0.18)
Coal combustion	median	0.246	0.296	0.227	0.19
	25th-75th percentile	(0.13–0.41)	(0.15–0.50)	(0.11–0.41)	(0.09–0.36)
Liquid fossil fuel combustion	median	0.459	0.534	0.598	0.638
	25th-75th percentile	(0.29–0.59)	(0.33–0.69)	(0.41–0.72)	(0.45–0.74)

Table S8. EC concentrations (in unit of μg m^{-3}) from biomass burning (EC_{bb}), coal combustion (EC_{coal}) and liquid fossil fuel combustion ($EC_{liq.fossil}$) for each sample (median and interquartile range in unit of μg m^{-3}), and the seasonal averaged concentrations (μg m^{-3}) calculated by averaging the median values for each sample in each season[a].

	EC_{bb}		EC_{coal}		$EC_{liq.fossil}$	
	median	(interquartile range)	median	(interquartile range)	median	(interquartile range)
Winter-H	3.07	(2.94–3.22)	2.79	(1.43–4.51)	4.03	(2.32–5.42)
Winter-M	1.44	(1.38–1.52)	1.42	(0.67–2.60)	3.25	(2.07–4.00)
Winter-L	0.82	(0.77–0.86)	0.69	(0.36–1.18)	1.28	(0.80–1.62)
Spring-H	0.36	(0.34–0.38)	1.02	(0.44–1.90)	1.81	(0.94–2.39)
Spring-M	0.30	(0.29–0.32)	0.70	(0.31–1.30)	1.29	(0.69–1.67)
Spring-L	0.22	(0.21–0.23)	0.50	(0.24–0.79)	0.57	(0.29–0.84)
Summer-H	0.32	(0.30–0.34)	0.66	(0.30–1.20)	1.20	(0.66–1.55)
Summer-M	0.17	(0.16–0.19)	0.20	(0.10–0.39)	0.61	(0.43–0.72)
Summer-L	0.12	(0.11–0.13)	0.16	(0.08–0.32)	0.42	(0.28–0.52)
Autumn-H	1.05	(1.00–1.10)	1.46	(0.68–2.99)	4.29	(2.80–5.08)
Autumn-M	0.54	(0.51–0.56)	0.68	(0.33–1.33)	2.58	(1.94–2.94)
Autumn-L	0.28	(0.26–0.29)	0.37	(0.18–0.68)	0.91	(0.60–1.11)
Winter[a]	1.78 ± 1.16		1.63 ± 1.06		2.86 ± 1.42	
Spring[a]	0.30 ± 0.07		0.74 ± 0.26		1.23 ± 0.62	
Summer[a]	0.20 ± 0.10		0.34 ± 0.28		0.75 ± 0.41	
Autumn[a]	0.62 ± 0.39		0.84 ± 0.57		2.59 ± 1.69	

[a]The seasonal averaged concentrations calculated by averaging the median values for each sample in each season.

References

Chow, J. C., Watson, J. G., Chen, L.-W. A., Chang, M. O., Robinson, N. F., Trimble, D., and Kohl, S.: The IMPROVE_A temperature protocol for thermal/optical carbon analysis: maintaining consistency with a long-term database, J. Air Waste Manage., 57, 1014–1023, 2007.

Zhao, Z., Cao, J., Zhang, T., Shen, Z., Ni, H., Tian, J., Wang, Q., Liu, S., Zhou, J., Gu, J., and Shen, G.: Stable carbon isotopes and levoglucosan for $PM_{2.5}$ elemental carbon source apportionments in the largest city of Northwest China, Atmos. Environ., 185, 253-261, https://doi.org/10.1016/j.atmosenv.2018.05.008, 2018.